JOURNAL OF AGRICULTURAL AND FOOD CHEMISTRY

Article

pubs.acs.org/JAFC

Multispectroscopic and Molecular Modeling Approach To Investigate the Interaction of Flavokawain B with Human Serum Albumin

Shevin R. Feroz,[†] Saharuddin B. Mohamad,[‡,§] Noraini Bujang,[§] Sri N.A. Malek,[†] and Saad Tayyab*[,†,§]

[†]Biomolecular Research Group, Biochemistry Programme, Institute of Biological Sciences, Faculty of Science, University of Malaya, 50603 Kuala Lumpur, Malaysia

[‡]Bioinformatics Programme, Institute of Biological Sciences, Faculty of Science, University of Malaya, 50603 Kuala Lumpur, Malaysia

[§]Centre of Research for Computational Sciences and Informatics for Biology, Bioindustry, Environment, Agriculture and Healthcare (CRYSTAL), Institute of Biological Sciences, Faculty of Science, University of Malaya, 50603 Kuala Lumpur, Malaysia

Supporting Information

ABSTRACT: Interaction of flavokawain B (FB), a multitherapeutic flavonoid from *Alpinia mutica* with the major transport protein, human serum albumin (HSA), was investigated using different spectroscopic probes, i.e., intrinsic, synchronous, and three-dimensional (3-D) fluorescence, circular dichroism (CD), and molecular modeling studies. Values of binding parameters for FB−HSA interaction in terms of binding constant and stoichiometry of binding were determined from the fluorescence quench titration and were found to be 6.88×10^4 M^{-1} and 1.0 mol of FB bound per mole of protein, respectively, at 25 °C. Thermodynamic analysis of the binding data obtained at different temperatures showed that the binding process was primarily mediated by hydrophobic interactions and hydrogen bonding, as the values of the enthalpy change (ΔH) and the entropy change (ΔS) were found to be −6.87 kJ mol^{-1} and 69.50 J mol^{-1} K^{-1}, respectively. FB binding to HSA led to both secondary and tertiary structural alterations in the protein as revealed by intrinsic, synchronous, and 3-D fluorescence results. Increased thermal stability of HSA in the presence of FB was also evident from the far-UV CD spectral results. The distance between the bound ligand and Trp-214 of HSA was determined as 3.03 nm based on the Förster resonance energy transfer mechanism. Displacement experiments using bilirubin and warfarin coupled with molecular modeling studies assigned the binding site of FB on HSA at domain IIA, i.e., Sudlow's site I.

KEYWORDS: *Alpinia mutica, flavokawain B, human serum albumin, ligand binding, molecular modeling, three-dimensional fluorescence*

INTRODUCTION

Plants serve as an immensely diverse source of bioactive compounds, important to both food and pharmaceutical industries. In recent times, plant-derived compounds, especially polyphenolic secondary metabolites and flavonoids, have attracted much attention due to their applications in the development of functional food products, dietary supplements, and new drugs.[1] The beneficial biological activities attributed to flavonoids include, but are not limited to, antioxidant, antiinflammatory, anticancer, antimicrobial, antidermatophytic, immunostimulating, hepatoprotective, and antinociceptive activities.[2−4]

Many plants under the genus *Alpinia* are frequently incorporated in human diets in many Asian countries because of their medicinal properties.[5] Parts of these plants are used as spices and food flavoring in cooking, ingredients in the preparation of traditional remedies and even eaten raw.[5] One of the several bioactive compounds recently isolated and characterized from *Alpinia mutica* in our laboratory is flavokawain B (FB), which belongs to the chalcone family of flavonoids (Figure 1).[6] Several studies have confirmed FB as a potent antiinflammatory,[5] anticancer,[6−8] and antinociceptive[9] agent based on inhibition of the nitric oxide synthase and cyclooxygenase pathways,[5] antiproliferation, and apoptosis of squamous, colon, and prostate cancer cell lines and chemical/thermal models of nociception in mice, respectively.[6−8]

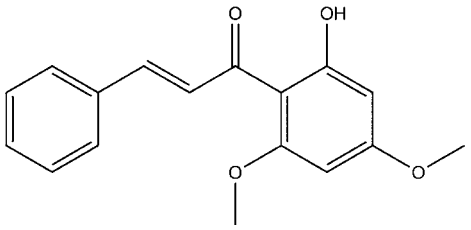

Figure 1. Chemical structure of flavokawain B.

The pharmacokinetics and pharmacodynamics of a particular drug in the human system are greatly affected by its interaction with plasma proteins, as the bioavailability, distribution, and metabolism of biologically active compounds (drugs or natural products) in the body are associated with their affinities to bind to transport proteins of mammalian blood circulation.[10,11] Protein-bound molecules possess prolonged times of action due to their protection from being metabolized and slow release

Received: March 15, 2012
Revised: May 24, 2012
Accepted: May 24, 2012
Published: May 24, 2012

into the target site.[12] Furthermore, drug−protein interaction may also have an influence on the structure of the protein.[13] Thus, the study on the interactions of ligands with proteins at the molecular level is important in understanding the action of these molecules in the body.

Human serum albumin (HSA) functions as the major transport and depot protein for a large number of endogenous and exogenous ligands.[10−13] It is a single-chain polypeptide made up of 585 amino acid residues, organized into three domains in a heart-shaped molecule.[10−13] The majority of the ligands bind to either of the two high affinity binding sites available on HSA, i.e., Sudlow's site I or site II, located in subdomains IIA and IIIA, respectively.[14] The presence of a solitary tryptophan residue (Trp-214) located in the subdomain IIA offers an advantage to studying the ligand binding process using fluorescence spectroscopy.[10]

In view of the above, we characterized the binding of FB to HSA using a multispectroscopic approach to describe the binding properties and the effect of the complexation on the protein structure. Ligand displacement and docking studies were also performed to characterize the FB binding site on HSA and the mode of binding.

MATERIALS AND METHODS

Materials. Human serum albumin (HSA), essentially fatty acid-free, warfarin (98% purity), and bilirubin (BR) were purchased from Sigma-Aldrich Inc., St. Louis, MO. Diazepam was supplied by Lipomed AG, Arlesheim, Switzerland. Flavokawain B (FB) was isolated and purified using procedures described elsewhere.[6] All other chemicals used were of analytical grade purity.

Analytical Procedures. Protein and warfarin stock solutions were prepared in 10 mM Tris-HCl buffer, pH 7.4, and methanol, respectively, and filtered through 0.45 μm Millipore filters, and their concentrations were determined spectrophotometrically using $E_{1\,cm}^{1\%}$ of 5.3 at 280 nm[15] and $E_{1\,cm}^{1\,M}$ of 13 610 at 310 nm,[16] respectively.

Stock BR solution was prepared by dissolving a few crystals in 1 mL of 0.5 M NaOH containing 1 mM EDTA[17] before diluting it to 50 mL with 10 mM Tris-HCl buffer, pH 7.4, and its concentration was determined spectrophotometrically using $E_{1\,cm}^{1\,M}$ of 47 500 at 440 nm.[18] BR solution was protected from light to avoid photodegradation and used within 1 h after preparation. All experiments involving BR were performed under dim light.

Diazepam stock solution was prepared by dissolving 10 mg of the drug in 10 mL of ethanol while a working solution was made by diluting 0.71 mL of the stock solution to 50 mL with the above buffer.

FB stock solution was prepared by dissolving 10 mg of FB crystals in 10 mL of 0.5 M NaOH whereas 1.42 mL of the stock solution was diluted to 50 mL with the above buffer to prepare a working solution.

Fluorescence Spectroscopy. Fluorescence measurements were made on a Jasco FP-6500 spectrofluorometer using a quartz cuvette of 1 cm path length, in a thermostatically controlled cell holder attached to a Protech 632D circulating water bath. The excitation and emission bandwidths were set at 10 nm each while the sensitivity, the response time, and the scan speed were fixed at 250 V, 2 s, and 500 nm min^{-1}, respectively. Intrinsic fluorescence of the protein solutions were measured upon exciting the samples at 280 nm and recording the emission spectra in the wavelength range of 300−380 nm.

Synchronous fluorescence spectra of the protein samples were obtained after scanning them in the wavelength range of 280−320 nm and 310−370 nm for the difference between excitation and emission wavelengths ($\Delta\lambda$) of 15 and 60 nm, respectively. The final protein concentration in each sample was 3 μM while FB concentrations were varied from 0.6 to 12 μM.

Three-dimensional (3-D) fluorescence spectra of HSA (3 μM) and the FB−HSA complexes (2:1 and 4:1 molar ratios) were obtained by using an excitation wavelength range of 220−350 nm with 10 nm increments and monitoring the emission spectra between 220 and 500 nm. The number of scanning curves was 14.

Circular Dichroism (CD) Spectroscopy. A Jasco J-815 spectropolarimeter was used for CD measurements after calibrating it with D-10-camphorsulfonic acid under a constant nitrogen flow. For experiments involving the FB−HSA complex, the protein solution (3 μM) containing 12 μM FB was incubated for 1 h at 25 °C for equilibrium attainment. For thermal stability studies, ellipticity values at 222 nm of the protein solution both in the absence and presence of FB were recorded in the temperature range of 25−100 °C followed by temperature reversal using a 1 mm path length cell regulated by a Jasco PTC-423S/15 temperature controller, connected to a Protech 632D circulating water bath. The samples were allowed to equilibrate for 6 min at each temperature in the given temperature range before CD measurements. CD values were transformed into mean residue ellipticity at 222 nm ($MRE_{222\,nm}$) values in the same way as described previously[19] and plotted against temperature.

Ligand Binding Studies. Binding of FB to HSA was studied using fluorescence spectroscopy. In titration experiments, HSA concentration was fixed at 3 μM while varying FB concentrations in the range of 1.5−22.5 μM in a total volume of 3 mL. After an incubation time of 1 h at 25 °C, fluorescence spectra were recorded in the same as way as described above. To study the effect of temperature on the FB−HSA interaction, titration experiments were carried out at three different temperatures, viz. 15 °C, 25 °C, and 35 °C, by recording the fluorescence intensity after an equilibration time of 6 min at each temperature. Values of the fluorescence intensity were transformed into relative fluorescence intensity by taking the fluorescence intensity of HSA in the absence of FB as 100.

The fluorescence data were analyzed using the Stern−Volmer equation:[20]

$$\frac{F_0}{F} = K_{SV}[Q] + 1 = k_q\tau_0[Q] + 1 \quad (1)$$

where the different terms have their usual significance.[20] The value of τ_0 was taken as 10^{-8} s for HSA in k_q calculation.[20] The modified Stern−Volmer equation was also used to determine the binding affinity between FB and HSA:[20]

$$\frac{F_0}{F_0 - F} = \frac{1}{K_a f_a [Q]} + \frac{1}{f_a} \quad (2)$$

where K_a and f_a are the association constant and fraction of the accessible fluorescence, respectively.

Binding data at different temperatures were used to analyze the thermodynamic parameters using the van't Hoff equation:[15]

$$\ln K = -\frac{\Delta H}{RT} + \frac{\Delta S}{R} \quad (3)$$

where K is the association constant, T is the absolute temperature, and R is the gas constant (8.3145 J mol^{-1} K^{-1}). Values of the enthalpy change (ΔH) and the entropy change (ΔS) were obtained from the slope and intercept, respectively, of the van't Hoff plot between ln K and $1/T$. Subsequently, the free energy change (ΔG) of the reaction at different temperatures was calculated by substituting the values of ΔH and ΔS thus obtained, into the equation, $\Delta G = \Delta H - T\Delta S$.

Fluorescence Resonance Energy Transfer. In the case of a significant overlap between the fluorescence emission spectrum of the donor (HSA) and the UV absorption spectrum of the acceptor (FB), the efficiency of the energy transfer E can be calculated according to the Förster's energy transfer theory using the following equation:[20]

$$E = 1 - \frac{F}{F_0} = \frac{R_0^6}{R_0^6 + r^6} \quad (4)$$

where F and F_0 are the fluorescence intensities of HSA in the presence and absence of FB and r is the distance between the donor and the acceptor. R_0 is the critical distance when the efficiency of the transfer is 50%, and its value in angstroms can be obtained with the help of the following relationship:[20]

$$R_0 = 9.78 \times 10^3[(k^2 n^{-4} Q_D J(\lambda)]^{1/6} \quad (5)$$

where k^2 is the spatial orientation factor between the emission dipole of the donor and the absorption dipole of the acceptor, and its value is taken as 2/3 for random orientations as found in fluid state; n is the average refractive index of the medium in the wavelength range of spectral overlap (1.336 in the present case[21]), Q_D is the fluorescence quantum yield of the donor in the absence of the acceptor (0.118 for HSA[21]), and J is the overlap integral of the emission spectrum of the donor and absorption spectrum of the acceptor. Values of J and R_0 were calculated using LabVIEW 8.2 (National Instruments Corp., Austin, TX) after integrating the emission spectrum of HSA and the absorption spectrum of FB, along with the values of k^2, n, and Q_D.

Competitive Ligand Displacement. BR displacement studies were carried out by recording the CD spectra of BR−HSA (1:1) complex (10 μM each) in the wavelength range of 300−500 nm both in the absence and presence of increasing FB concentrations (15−75 μM) using a scan speed of 100 nm min^{-1}. BR−HSA solutions were first incubated for 15 min at 25 °C (sufficient for equilibrium attainment) in the dark prior to the addition of FB, followed by another 15 min of incubation before CD spectral measurements.

To study the displacement of warfarin in the presence of FB, emission fluorescence spectra of warfarin−HSA (1:1) complex (3 μM each) were recorded in the wavelength range of 360−520 nm upon excitation at 335 nm both in the absence and presence of increasing FB concentrations (3−24 μM) under experimental conditions similar to that described above. Warfarin−HSA mixtures were preincubated for 1 h at 25 °C prior to the addition of FB. This was followed by another 1 h of equilibration before the spectra were recorded.

Site-specific experiments using diazepam were performed by titrating 3 μM HSA and FB−HSA mixture (3:1) with increasing concentrations of diazepam (0−6 μM). The fluorescence spectra of HSA were recorded between 300−380 nm upon excitation at 280 nm.

Molecular Modeling. The structure of FB was constructed using ACD/ChemSketch Freeware (Advanced Chemistry Development Inc., Ontario, Canada), 3D optimized, and exported as a mol file. The geometry optimization of FB was refined with the VegaZZ 2.08[22] batch processing MOPAC script (mopac.r; keywords: MMOK, PRECISE, GEO-OK) using AM1 semiempirical theory[23] and then converted and stored as a mol2 file. Docking, visualization, and rendering simulation were performed using AutoDock[24] and AutoDockTools 1.5.4[25] at the Academic Grid Malaysia Infrastructure. The crystal structure of HSA (PDB code 1BM0, 2.5 Å resolution) was downloaded from the Protein Data Bank.[26] Water molecules were removed, and the atomic coordinates of chain A of 1BM0 were stored in a separate file and used as input for AutoDockTools. Thus, polar hydrogens, Kollman charges, and solvation parameters were added. In the case of the ligand FB, nonpolar hydrogens were merged and rotatable bonds were defined. The two binding sites (subdomains IIA and IIIA) were defined using two grids of 70 × 70 × 70 points each with a grid space of 0.375 Å centered at coordinates x = 35.26, y = 32.41, and z = 36.46 for subsite IIA and x = 14.42, y = 23.55, and z = 23.31 for subsite IIIA, respectively. Lamarckian genetic algorithm with local search was used as the search engine, with a total of 100 runs for each binding site. In each run, a population of 150 individuals with 27 000 generations and 250 000 energy evaluations were employed. Operator weights for crossover, mutation, and elitism were set to 0.8, 0.02, and 1, respectively. For the local search, default parameters were used. Cluster analysis was performed on docked results using a root-mean-square deviation (rmsd) tolerance of 2.0 Å. The protein−ligand complex was visualized and analyzed using AutoDockTools.

Statistical Analysis. Curve fitting and processing of statistical data were performed using the OriginPro 8.5 software (OriginLab Corp., Northampton, MA).

RESULTS AND DISCUSSION

FB-Induced Quenching of HSA Fluorescence and Binding Parameters. Fluorescence quenching or a decrease in the fluorescence intensity of a system can be explained by a variety of molecular interactions such as excited-state reactions, molecular rearrangement, energy transfer, ground-state complex formation, and collisional quenching.[20] HSA produced a fluorescence spectrum in the wavelength range of 300−380 nm with an emission maxima at 337 nm when excited at 280 nm (Figure 2). This was in accordance with earlier reports[19,27,28]

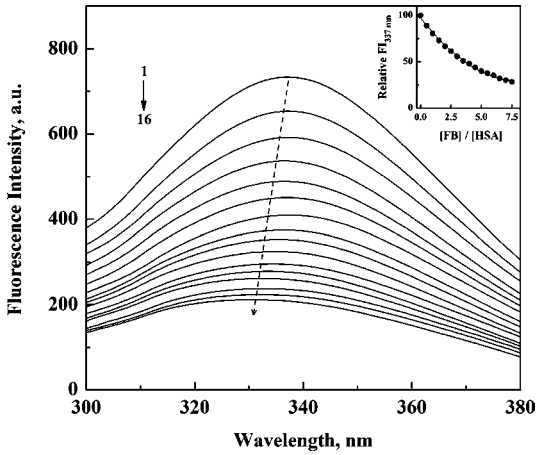

Figure 2. Fluorescence spectra of HSA in the absence and presence of increasing FB concentrations, obtained in 10 mM Tris-HCl buffer, pH 7.4, at 25 °C upon excitation at 280 nm. The concentration of HSA was 3 μM, whereas FB concentrations (from top to bottom, 1−16) were 0−22.5 μM at regular increments of 1.5 μM. The inset shows the decrease in the relative fluorescence intensity at 337 nm ($FI_{337\ nm}$) against FB/HSA molar ratio.

and can be ascribed to the presence of a single Trp residue in the protein. Addition of FB led to a concentration-dependent quenching of the intrinsic fluorescence of HSA along with a blue shift of 6 nm in its emission maxima. The decrease in the fluorescence intensity of HSA upon addition of FB was more pronounced at lower FB/HSA molar ratios and sloped off at higher molar ratios (inset of Figure 2). About 72% quenching was observed at a FB/HSA molar ratio of 7.5. Increased hydrophobicity around the fluorophore(s) can account for the blue shift in the emission maxima, whereas movement of charged groups as well as hydrophobic changes in the microenvironment around fluorophore(s) are responsible for the decrease in the fluorescence intensity.[29] These changes in the fluorescence properties of HSA reflected conformational alterations in the three-dimensional structure of the protein upon FB addition and therefore suggested the binding of FB to HSA.

To characterize the mechanism of the fluorescence quenching involved in the FB−HSA system, quenching experiments were performed at three different temperatures, i.e., 288 K, 298 K, and 308 K. Figure 3A shows the Stern−Volmer plots for the FB−HSA system obtained at these temperatures. It should be noted that the plots showed an upward deviation at higher FB concentrations. This was not unusual, as many reports have shown upward deviation in the Stern−Volmer plots.[30−32] Therefore, results at lower ligand concentrations, showing linearity were selected for regression analysis. Values of K_{SV} were obtained from the slope of these plots and are listed in Table 1. As can be seen from the table, an inverse correlation between K_{SV} and temperature was noticed. Because static quenching is characterized by the decrease in the quenching constant with the increase in temperature,[20] our

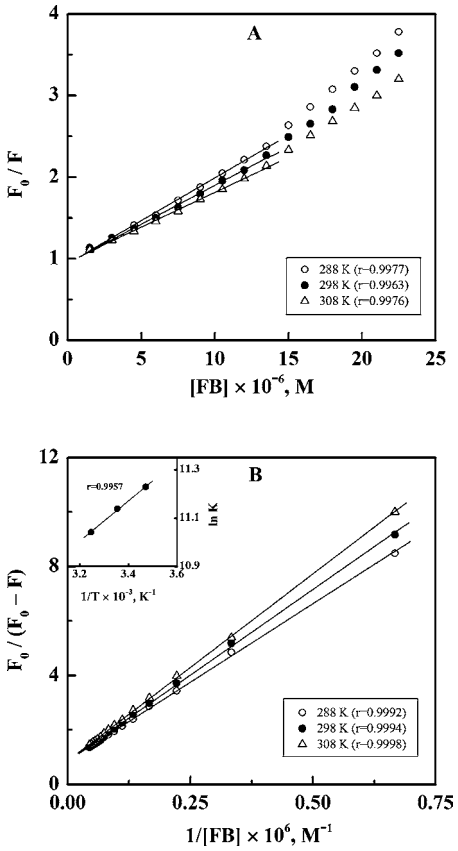

Figure 3. (A) Stern–Volmer plots for fluorescence quenching data of the FB–HSA system at three different temperatures, i.e., 288 K, 298 K, and 308 K. (B) Modified Stern–Volmer plots for fluorescence quenching data of the FB–HSA system at three different temperatures as mentioned in A. The inset shows the van't Hoff plot for FB–HSA interaction.

results suggested that the quenching of HSA fluorescence by FB was due to the formation of a complex. Furthermore, larger k_q values (1.05×10^{13}, 0.95×10^{13} and 0.85×10^{13} M^{-1} s^{-1} at 288 K, 298 K, and 308 K, respectively) obtained for the FB–HSA system compared to the highest value reported for a diffusion-controlled process (2.0×10^{10} M^{-1} s^{-1}) also opposed the involvement of dynamic quenching in the binding process.[33] Thus, the overall quenching of HSA fluorescence by FB can be best described by the static quenching mechanism.

In view of the involvement of static quenching in the FB–HSA system, quenching data were also analyzed following the modified Stern–Volmer equation (see Materials and Methods) and the obtained plots at three different temperatures are shown in Figure 3B. It is important to note that all points in the modified Stern–Volmer plots had fallen on the straight line as shown in Figure 3B (correlation coefficient ~0.999), when compared to the Stern–Volmer plots (Figure 3A). Values of K_a, obtained by dividing the y-intercept with the slope for each plot, are listed in Table 1. Similar values of K_a, falling in the range of $1–15 \times 10^4$ M^{-1}, have been reported for a large number of ligands, binding to HSA, using fluorescence spectroscopy.[3,21,28,31,32] The trend of decreasing K_a values with increasing temperature was similar to that observed with the K_{SV} values. This can be explained on the basis of destabilization of the FB–HSA complex at higher temperatures and supported the static quenching mechanism for the FB–HSA system. Moderate affinity of a compound toward a protein helps in the diffusion of the compound from the circulatory system to reach its target site. Such a value of K_a obtained for FB binding to HSA fulfills this criterion for its transport in the blood circulation and diffusion at the target site.

Assuming the binding of FB as independent to a set of equivalent sites on HSA, the number of binding sites, n, was determined from the slope of the plots between log $((F_0 - F)/F)$ versus log Q[34] (Supporting Information Figure 1) obtained at different temperatures and were found to be 1.14, 1.13, and 1.11 at 288 K, 298 K, and 308 K, respectively. These results suggested the presence of a single class of FB binding sites on the HSA molecule.

Thermodynamic Parameters and Acting Forces. To characterize the forces involved in the FB–HSA interaction, thermodynamic parameters for the binding reaction were determined from the van't Hoff plot (inset of Figure 3B) and are listed in Table 1. The negative ΔH and positive ΔS values contributed significantly toward making the ΔG value more negative for the reaction (Table 1) and therefore suggested the formation of a complex between FB and HSA as the most favorable one.

For a number of processes involving hydrophobic interactions, values of ΔS were found to be positive whereas ΔH values were either close to zero or negative.[35,36] Binding of the ligand to the protein molecule leads to the burial of water-accessible surface area of the protein, which in turn releases the solvent from the surface. As a result, the system acquires a favorable entropic change which is reflected by the positive ΔS value. In view of this, the binding phenomenon between FB and HSA is supposed to involve mainly hydrophobic interactions. This seems understandable, as FB possesses benzenoid character as well as several nonpolar groups which can interact with the protein's hydrophobic residues. Although electrostatic forces are also governed by a positive ΔS value, ΔH has been found to be either very small or close to zero for these forces.[37] In the presence of the high negative ΔH value obtained, involvement of electrostatic force in the FB–HSA interaction remains questionable. Moreover, FB lacks the presence of any ionizable group through which it can participate via electrostatic force in the binding process. A significantly higher pK value of the phenolic hydroxyl group in FB molecule might have prevented its ionization at pH 7.4 to participate in electrostatic interactions. A negative ΔH value obtained may also account for the involvement of hydrogen bonding in this interaction.[35,36] It would be an over-simplification to presume the involvement of a single force in

Table 1. Binding and Thermodynamic Parameters of the FB–HSA System at pH 7.4

T (K)	K_{sv} (M^{-1})	K_a (M^{-1})	$\Delta S°$ (J mol^{-1} K^{-1})	$\Delta H°$ (kJ mol^{-1})	$\Delta G°$ (kJ mol^{-1})
288	1.05×10^5	7.52×10^4			−26.89
298	0.95×10^5	6.88×10^4	69.50	−6.87	−27.59
308	0.85×10^5	6.24×10^4			−28.28

dx.doi.org/10.1021/jf301139h | J. Agric. Food Chem. 2012, 60, 5899–5908

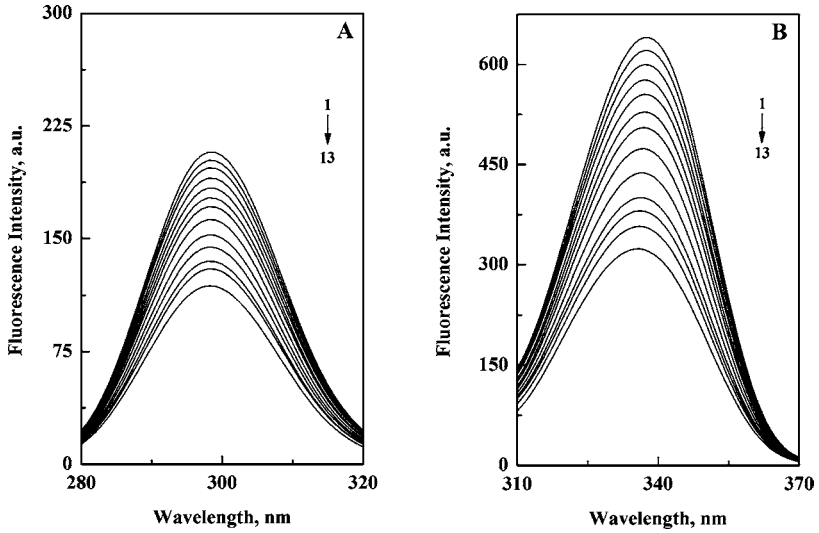

Figure 4. Synchronous fluorescence spectra of HSA in the absence and presence of increasing FB concentrations at 25 °C, obtained in 10 mM Tris-HCl buffer, pH 7.4. The concentration of HSA was kept constant at 3 μM while FB concentrations were varied (from top to bottom, 1−13): 0, 0.6, 1.2, 1.8, 2.4, 3, 4.2, 5.4, 6.6, 7.8, 9, 10.5, and 12.0 μM. (A) $\Delta\lambda$ = 15 nm, (B) $\Delta\lambda$ = 60 nm.

the ligand−protein interaction. Hence, both hydrophobic force and hydrogen bonding seem to play the major role in FB−HSA interaction.

Synchronous Fluorescence. Alteration in the microenvironment around the fluorophores (Tyr and Trp) in the three-dimensional structure of HSA upon FB binding was elucidated by synchronous fluorescence spectra. Figure 4A and 4B shows the effect of increasing concentrations of FB on the synchronous fluorescence spectra of HSA at the $\Delta\lambda$ value of 15 and 60 nm, respectively. While no change in the emission maxima (298 nm) was observed upon addition of FB when $\Delta\lambda$ was 15 nm, synchronous fluorescence spectra obtained with $\Delta\lambda$ = 60 nm showed a blue shift from 338 to 336 nm upon FB addition. These results suggested that binding of FB to HSA had little effect on the microenvironment around Tyr residues but was sufficient to perturb the environment in the vicinity of the lone Trp residue (Trp-214), located in subdomain IIA, from polar to slightly nonpolar.

Three-Dimensional Fluorescence. To gain more insight about the conformational changes in HSA upon FB binding, three-dimensional (3-D) fluorescence spectroscopy was performed on HSA both in free form and in the presence of FB. Figure 5 shows 3-D fluorescence spectra and the corresponding contour maps of native HSA (A and A′) and HSA in the presence of FB with FB/HSA molar ratios of 2:1 (B and B′) and 4:1 (C and C′). The 3-D fluorescence spectral characteristics in terms of peak position ($\lambda_{ex}/\lambda_{em}$) and intensity are listed in Table 2. Two peaks, namely, a and b, referring to the Rayleigh scattering peak ($\lambda_{ex} = \lambda_{em}$) and the second-order scattering peak ($2\lambda_{ex} = \lambda_{em}$), respectively, were common in all spectra.[38] It is important to note that both these scattering peaks were also present in the 3-D fluorescence spectra of the buffer (Supporting Information Figure 2). In addition to both scattering peaks, protein samples in the absence and presence of FB showed two (1 and 2) and three (1, 2, and 3) additional peaks, respectively. Peak 1 (λ_{ex} = 280 nm, λ_{em} = 337 nm) represented the intrinsic fluorescence characteristics of HSA due to Trp and Tyr residues involving $\pi \rightarrow \pi^*$ transition and reflected changes in the tertiary structure of HSA upon complexation with FB. On the other hand, peak 2 (λ_{ex} = 230 nm, λ_{em} = 332 nm) was related to the fluorescence characteristics of the polypeptide backbone structure of HSA caused by the $\pi \rightarrow \pi^*$ transition and reflected changes in the secondary structure of HSA in the presence of FB.[38] Presence of peak 3 obtained in the presence of FB represented the fluorescence characteristics due to FB. Addition of FB to the protein solution in a molar ratio of 2:1 produced a significant decrease in the intensity along with a blue shift in both peaks 1 and 2, being ∼36%, 1 nm, and 33%, 6 nm, respectively. Increasing the molar ratio of FB/HSA to 4:1 aggravated these changes further to 60%, 2 nm, and 52%, 11 nm, respectively. Changes in the 3-D fluorescence spectral characteristics of peak 1 were similar to synchronous fluorescence results (Figure 4), suggesting perturbation in the tertiary structure of HSA in the presence of FB whereas 3-D fluorescence spectral results of peak 2 indicated secondary structural alteration in the protein upon FB binding.

Thermal Stability. CD spectroscopy was employed to study the effect of FB binding to HSA on its thermal stability by determining the loss in the $MRE_{222\ nm}$ value of HSA with increasing temperature (25−100 °C) both in the absence and presence of FB. Thermal denaturation curves of HSA and the FB−HSA complex showed similar cooperative transition up to 90 °C, beyond which there was a steep loss in $MRE_{222\ nm}$ of HSA against a gradual decrease in the $MRE_{222\ nm}$ value observed with the FB−HSA complex (Figure 6A). To validate these findings, cooling experiments were performed in the same way after equilibration of the samples for 6 min at each temperature in the reverse order. As can be seen from Figure 6A, HSA alone did not show any recovery in the $MRE_{222\ nm}$ value upon cooling and a clear precipitate was noticed at 25 °C in the reversibility experiment. These results suggested irreversible structural changes leading to aggregation in HSA at high temperatures and agreed well with earlier reports.[15,39] Contrary to it, a significant increase in $MRE_{222\ nm}$ signal from −40 at 100 °C to −60 at 25 °C was observed with the FB−HSA complex and the solution remained clear upon cooling to 25 °C. Both these results suggested relatively higher thermal stability of HSA in the presence of FB which not only prevented precipitation but also produced a significant reversal

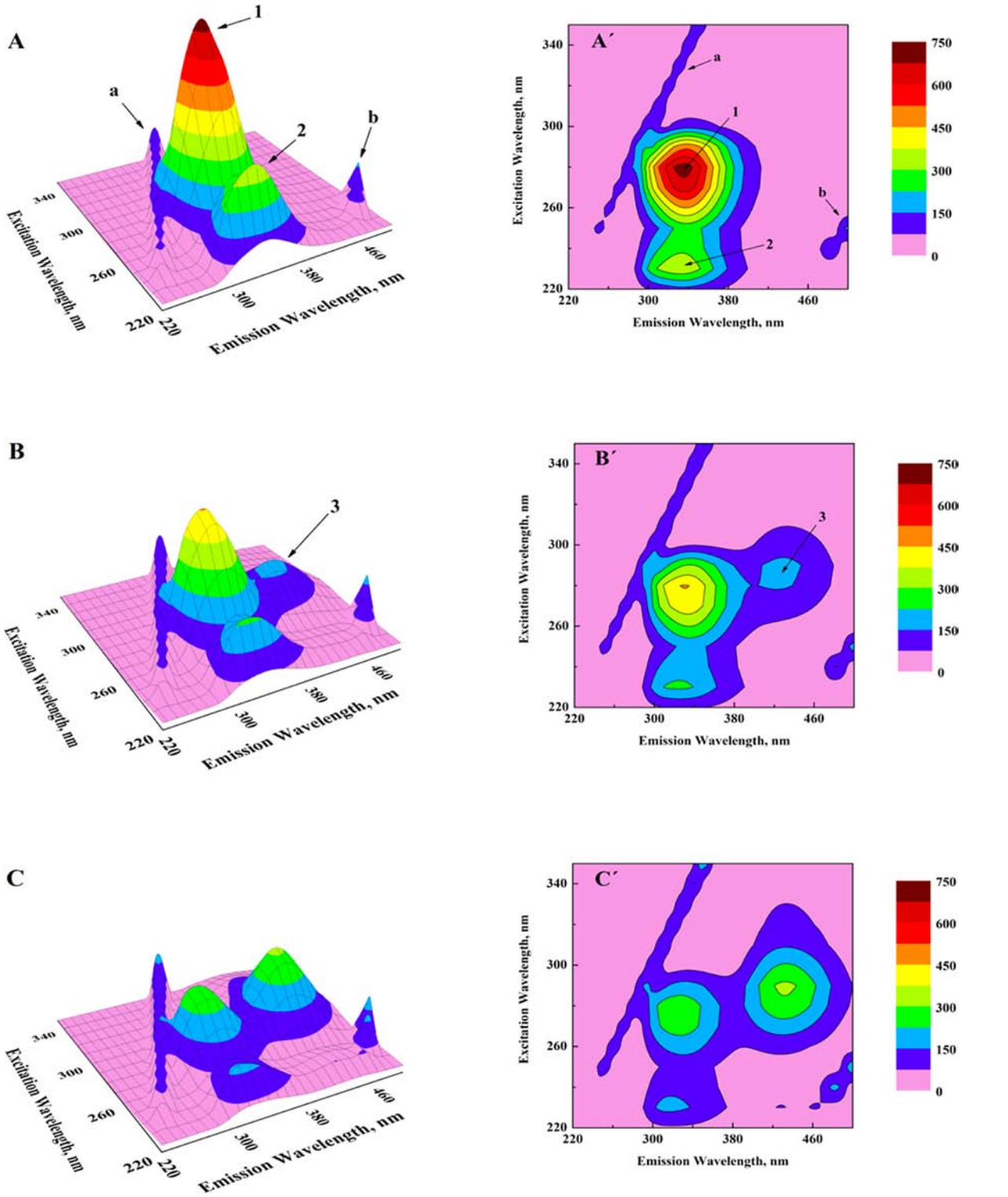

Figure 5. Three-dimensional fluorescence spectra (A–C) and corresponding contour maps (A′–C′) of HSA (A and A′) and FB–HSA systems ([FB]/[HSA] = 2:1 (B and B′), 4:1 (C and C′)) at 25 °C, obtained in 10 mM Tris-HCl buffer, pH 7.4.

in the $MRE_{222\ nm}$ value upon cooling. The thermal denaturation/renaturation of HSA in the absence and presence of FB were also studied within the temperature range 25–80 °C, and the results are shown in Figure 6B. Although thermal denaturation curves of HSA and the FB–HSA complex showed a similar pattern, a significant difference was observed in the reversibility experiments. Whereas both solutions remained clear upon cooling, the FB–HSA complex exhibited a higher extent of recovery in terms of $MRE_{222\ nm}$ compared to HSA alone. These results further suggested the stabilizing effect of bound FB on HSA against heat treatment. This was in accordance with previous reports suggesting higher thermal stability of HSA upon ligand binding.[40,41]

dx.doi.org/10.1021/jf301139h | J. Agric. Food Chem. 2012, 60, 5899–5908

Table 2. Three-Dimensional Fluorescence Spectral Characteristics of HSA and FB−HSA Systems at pH 7.4, 25 °C

system	peak no.	peak position [$\lambda_{ex}/\lambda_{em}$ (nm/nm)]	intensity
HSA	a	230/230→350/350	23.03→128.02
	b	250/500	165.38
	1	280/337	708.34
	2	230/332	359.12
[FB]:[HSA] = 2:1	a	230/230→350/350	24.06→153.48
	b	250/500	180.46
	1	280/336	453.91
	2	230/326	240.51
	3	290/428	169.92
[FB]:[HSA] = 4:1	a	230/230→350/350	24.79→181.44
	b	250/500	196.02
	1	280/335	280.52
	2	230/321	172.52
	3	290/432	315.32

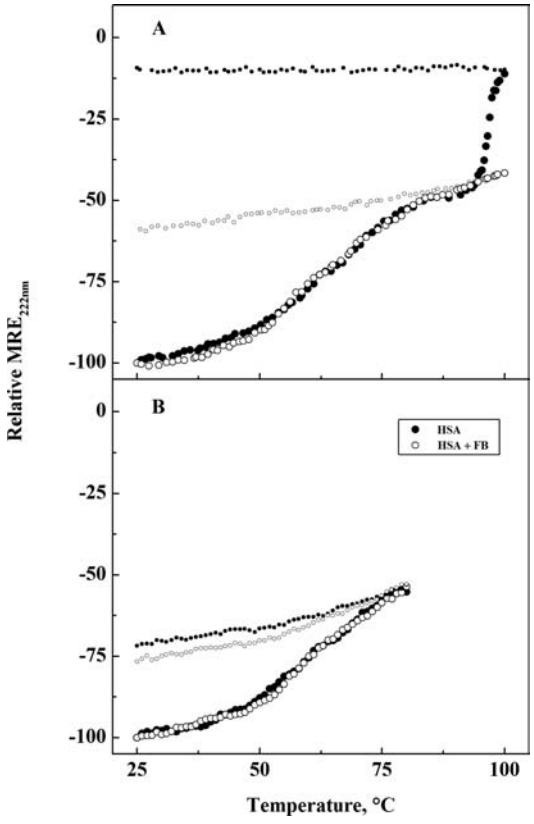

Figure 6. Thermal denaturation and renaturation curves of HSA and FB−HSA (4:1) complex as studied by $MRE_{222\ nm}$ measurements in the temperature range of (A) 25−100 °C and (B) 25−80 °C, obtained in 10 mM Tris-HCl buffer, pH 7.4. The concentrations of HSA and FB were 3 μM and 12 μM, respectively. Renaturation curves are shown with smaller symbols.

Fluorescence Resonance Energy Transfer and Binding Distance. Transfer of excitation energy from an excited donor fluorophore to a nearby acceptor results in the phenomenon of resonance energy transfer. This phenomenon is possible if the absorption spectrum of the acceptor overlaps the emission spectrum of the donor, the donor and the acceptor molecules are in close proximity (∼2−8 nm), and the donor and the acceptor transition dipole orientations are approximately parallel.[20] There was significant overlap between the emission spectrum of HSA and the absorption spectrum of FB (Supporting Information Figure 3), and therefore there is high probability of resonance energy transfer between HSA and FB. Using Förster's energy transfer theory, values of R_0, J, and E at a FB/HSA molar ratio of 1:1 were calculated as 2.387 nm, 8.56×10^{-15} M^{-1} cm^3, and 0.193, respectively. Substitution of the values of E and R_0 into eq 4 yielded a value of r (distance between the bound FB and Trp-214 of HSA) as 3.03 nm. The value of r thus obtained was found to lie within the permissible limits of the distance (2−8 nm) between the donor and the acceptor molecules, indicating the high probability of energy transfer between HSA and FB. Furthermore, the larger value of r in comparison to R_0 supported the static quenching mechanism for the interaction of FB with HSA as demonstrated earlier for other ligand−protein interactions.[28,34]

Site-Specific Binding of FB to HSA. Majority of the ligands have been shown to bind to either Sudlow's site I or site II of HSA, located in subdomains IIA and IIIA, respectively.[10] In view of this, displacement experiments were carried out using reporter ligands, BR and warfarin, for site I and diazepam for site II of HSA to establish the binding site of FB on HSA. Titration of HSA alone as well as its complex with FB (FB−HSA) with diazepam produced similar quenching results when studied by fluorescence spectroscopy (Supporting Information Figure 4), suggesting noninvolvement of site II of HSA in FB binding. On the other hand, displacement experiments with warfarin and BR proved successful in characterizing the FB binding site on HSA as site I.

Figure 7A shows the displacing action of FB on the BR−HSA (1:1) complex as studied by CD spectroscopy. BR upon binding to HSA acquired chirality and resulted in a Cotton effect, marked by a bisignate CD spectra in the wavelength range of 300−500 nm, with a negative peak at lower wavelength (407 nm) and a positive peak at higher wavelength (458 nm).[42] It is important to note that free BR, HSA, or FB solutions did not produce any CD spectral signal within this range (a, b, and c in Figure 7A). Addition of increasing concentrations (15−75 μM) of FB to BR−HSA complex led to a significant reduction in the CD spectral characteristics, suggesting displacement of BR from its binding site on HSA. The CD spectral signal at 458 nm obtained with the BR−HSA complex decreased continuously with increasing FB concentrations, showing 40% reduction at an FB/HSA molar ratio of 7.5:1 (inset of Figure 7A). Thus, the binding site of FB on HSA seemed to be located in the close vicinity of the BR binding site, i.e., site I.

To strengthen these findings, displacement experiments were also carried out with the warfarin−HSA complex using fluorescence spectroscopy. The warfarin−HSA (1:1) complex produced a fluorescence spectrum in the wavelength range of 360−520 nm with an emission maxima at 383 nm when excited at 335 nm (Figure 7B).[42] Addition of increasing FB concentrations (3−24 μM) to the warfarin−HSA complex produced a progressive decrease in the fluorescence intensity, which was indicative of warfarin displacement by FB. About 35% decrease in the fluorescence intensity was observed at an FB/HSA molar ratio of 8:1 (inset of Figure 7B). FB, a fluorescent compound also produced a fluorescence spectrum in the same wavelength range, when excited at 335 nm. However, the emission maxima was found to appear at 433 nm,

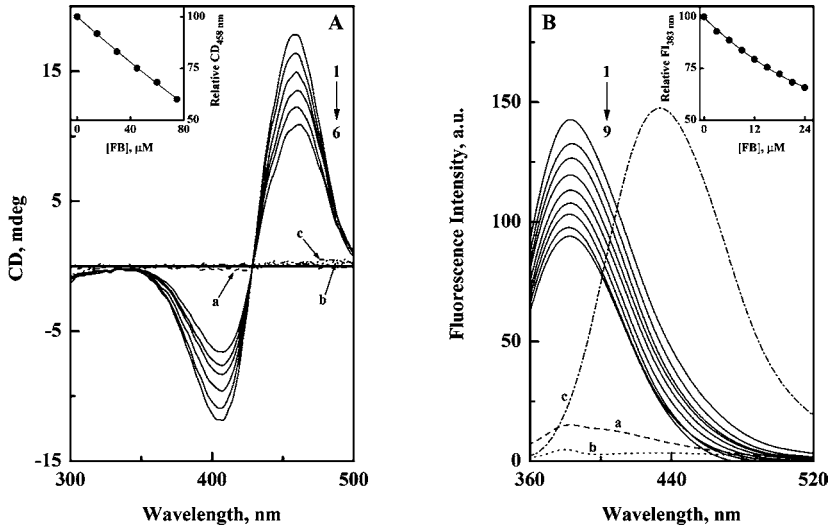

Figure 7. Displacing action of FB on the binding of site I drugs to HSA. (A) Effect of FB on the visible CD spectrum of BR−HSA (1:1) complex at 25 °C. The concentrations of BR and HSA were 10 μM each while the concentration of FB was varied (from top to bottom, 1−6): 0−75 μM at regular increments of 15 μM. CD spectra shown as a, b, and c refer to 10 μM BR, 10 μM HSA, and 75 μM FB, respectively. The inset shows the decrease in the relative CD value at 458 nm with increasing FB concentrations. (B) Effect of FB on the fluorescence spectrum of warfarin−HSA (1:1) complex at 25 °C. The concentrations of warfarin and HSA were 3 μM each while the concentration of FB was varied (from top to bottom, 1−9): 0−24 μM at regular increments of 3 μM. Emission spectra marked as a, b, and c refer to 3 μM warfarin, 3 μM HSA, and 24 μM FB, respectively. The inset shows the decrease in the relative fluorescence intensity at 383 nm ($FI_{383\ nm}$) with increasing FB concentrations.

far from the 383 nm signal (emission maxima) of the warfarin−HSA complex. Furthermore, both warfarin and HSA produced weak signals in the wavelength range studied. Taken together, displacement of BR as well as warfarin in the presence of FB suggested the binding of FB to Sudlow's site I of HSA.

Molecular Modeling. A molecular modeling study was conducted to predict the binding site of FB in HSA and to confirm the results of the displacement experiments described above. The ligand was constructed, geometrically optimized, and docked to the X-ray structure of HSA with high resolution (PDB code 1BM0). The binding mode of FB was predicted for the two main drug binding sites I and II (Sudlow's nomenclature;[14] at subdomains IIA and IIIA of HSA, respectively).

Cluster analysis was performed for the binding site I using a rmsd tolerance of 2.0 Å. A total of 9 multimember conformational clusters were obtained from 100 docking runs. The highest populated cluster contained more than half of the analyzed conformations (53 out of 100 conformations) and found to be the lowest on the energy scale. Hence, it was the most energetically favorable cluster, possessing an estimated docking energy of about −7.6 kcal mol^{-1} (Figure 8A). Whereas for the binding site II, using the same approach, about 26 distinct conformational clusters were obtained. However, the most populated cluster (14 out of 100 conformations) was not the most energetically favorable (−4.2 kcal mol^{-1}) cluster (Figure 8B). Accordingly, FB showed a binding preference for the drug binding site I (subdomain IIA) of HSA. The results of these docking studies were in good agreement with the displacement experiments discussed above.

The predicted binding model with the lowest docking energy (−7.6 kcal mol^{-1}) was then used for binding orientation analysis (Figure 9). The binding site (defined as amino acids within a 5 Å distance to FB) was found to be deep inside the protein structure and mostly located in a hydrophobic cleft lined by the following amino acids: Tyr-150, Glu-153, Ser-192, Lys-195, Gln-196, Lys-199, Leu-219, Leu-238, Arg-222, Val-241, His-242, Arg-257, Leu-260, Ala-261, Ile-264, Ser-287, His-288, Ile-290, Ala-291, and Glu-292. The interaction between FB and HSA cannot be presumed to be exclusively hydrophobic in nature, as there were several ionic as well as polar residues in the proximity of the bound ligand. Five hydrogen bonds were predicted from the conformation. These hydrogen bonds between the amino acid residues of HSA to the oxygen atom of

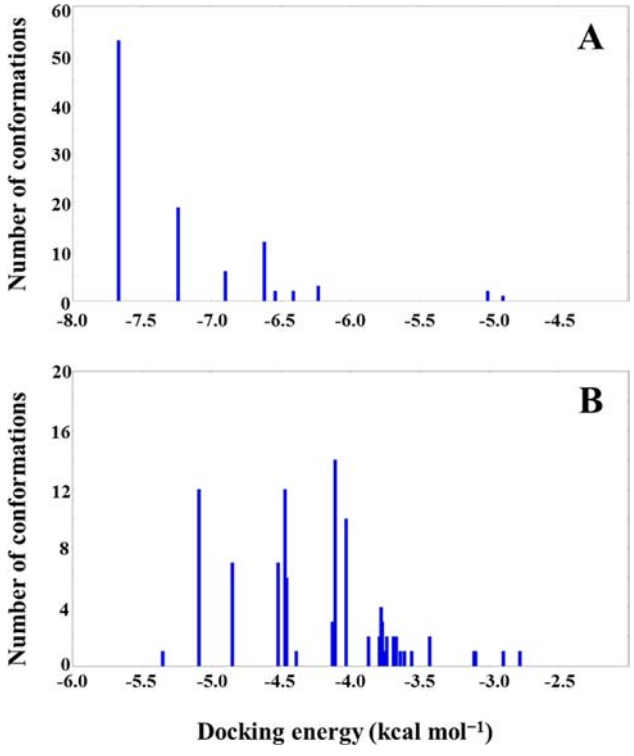

Figure 8. Cluster analyses of the AutoDock docking runs of FB in the drug binding site I (A) and site II (B) involving subdomains IIA and IIIA of HSA, respectively.

dx.doi.org/10.1021/jf301139h | J. Agric. Food Chem. 2012, 60, 5899−5908

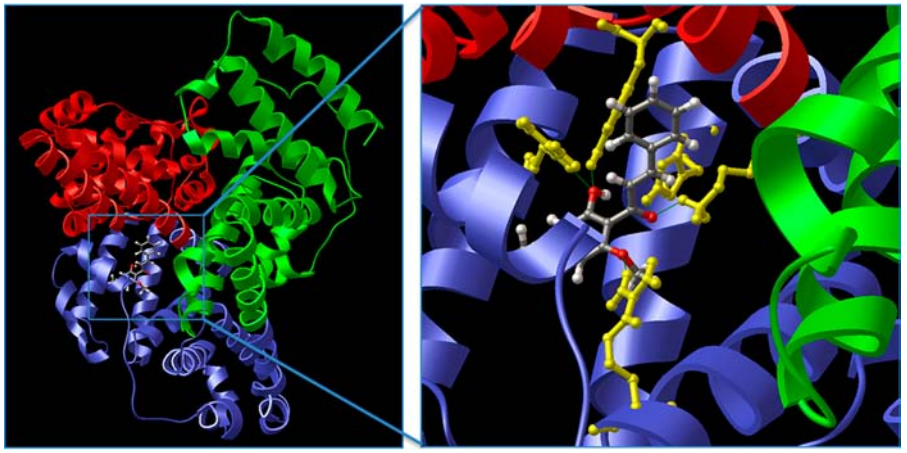

Figure 9. Predicted orientation of the lowest docking energy conformation of FB (ball and stick rendered) in the subdomain IIA (binding site I) of HSA. The domains of HSA are colored red for domain I, blue for domain II, and green for domain III. The binding site was enlarged to show hydrogen bonding (green lines) between the amino acid residues and FB. Amino acid residues that form hydrogen bonds with FB are rendered in ball and stick and colored yellow.

the hydroxyl, carbonyl, and methoxyl group of FB are summarized in Table 3. The benzene rings of the ligand seemed to be buried inside the hydrophobic cleft and stabilized the docking conformation through hydrophobic interactions with other hydrophobic residues of the protein clustered within the binding site.

Table 3. Hydrogen Bond Distance between Interacting Atoms of the Amino Acid Residues of HSA and FB

protein atom	FB atom	distance (Å)
Tyr-150: HH	O (hydroxyl)	1.758
Lys-199: HZ3	O (carbonyl)	1.925
Arg-222: HH11	O (methoxyl)	2.236
His-242: HE2	O (carbonyl)	2.095
Arg-257: HE	O (hydroxyl)	1.818

In conclusion, the interaction of FB with HSA was found to be comparable to many other flavonoids in terms of binding affinity and stoichiometry when investigated by fluorescence spectroscopy. The binding reaction mainly involved hydrophobic interactions as well as hydrogen bonding as revealed by thermodynamic parameters and docking studies. Binding of FB to HSA also led to structural changes in the protein as analyzed by intrinsic, synchronous, and three-dimensional fluorescence. Sudlow's site I of HSA, located in domain IIA, was assigned to be the most probable binding site for FB on HSA, as suggested by competitive ligand displacement experiments as well as computer modeling studies. These results will be helpful in understanding the pharmacokinetics and pharmacodynamics of FB.

■ ASSOCIATED CONTENT

Supporting Information

Supporting Information Figure 1: Double logarithmic plots for fluorescence quenching data of FB−HSA system at three different temperatures, i.e., 288 K, 298 K, and 308 K. Supporting Information Figure 2: Three-dimensional fluorescence spectra and corresponding contour map of 10 mM Tris-HCl buffer, pH 7.4. Supporting Information Figure 3: Spectral overlap between the emission spectrum of HSA and UV absorption spectrum of FB. Both spectra were recorded at 25 °C in 10 mM Tris-HCl buffer, pH 7.4. The concentrations of HSA and FB were 3 μM each. Supporting Information Figure 4: Fluorescence quenching of HSA and the FB−HSA complex by diazepam. This material is available free of charge via the Internet at http://pubs.acs.org.

■ AUTHOR INFORMATION

Corresponding Author

*Phone: +603 7967 7118. Fax: +603 7967 4178. E-mail: saadtayyab2004@yahoo.com.

Funding Sources

This work was financially supported by an HIR Grant (F000002-21001) approved by the Ministry of Higher Education, Government of Malaysia and the University of Malaya. S.R.F is working as a Research Assistant under this project funding.

Notes

The authors declare no competing financial interest.

■ ACKNOWLEDGMENTS

The authors thank the Dean, Faculty of Science and the Head, Institute of Biological Sciences, University of Malaya, for providing all the necessary facilities to carry out this work.

■ ABBREVIATIONS USED

FB, flavokawain B; HSA, human serum albumin; CD, circular dichroism; BR, bilirubin; MRE, mean residue ellipticity; rmsd, root-mean-square deviation

■ REFERENCES

(1) Eyheraguibel, B.; Richard, C.; Ledoigt, G.; Halle, A. T. Inhibition of herbicide photodegradation by plant products. *J. Agric. Food Chem.* **2011**, *59*, 4868−4873.

(2) Shi, S.; Zhang, Y.; Chen, X.; Peng, M. Investigation of flavonoids bearing different substituents on ring C and their Cu^{2+} complex binding with bovine serum albumin: Structure−affinity relationship aspects. *J. Agric. Food Chem.* **2011**, *59*, 10761−10769.

(3) Dufour, C.; Dangles, O. Flavonoid−serum albumin complexation: Determination of binding constants and binding sites by fluorescence spectroscopy. *Biochim. Biophys. Acta* **2005**, *1721*, 164−173.

(4) Tsuchiya, H. Structure-dependent membrane interaction of flavonoids associated with their bioactivity. *Food Chem.* **2010**, *120*, 1089−1096.
(5) Lin, C. T.; Kumar, K. J. S.; Tseng, Y. H.; Wang, Z. J.; Pan, M. Y.; Xiao, J. H.; Chien, S. C.; Wang, S. Y. Anti-inflammatory activity of flavokawain B from *Alpinia pricei* Hayata. *J. Agric. Food Chem.* **2009**, *57*, 6060−6065.
(6) Malek, S. N. A.; Phang, C. W.; Ibrahim, H.; Wahab, N. A.; Sim, K. S. Phytochemical and cytotoxic investigations of *Alpinia mutica* rhizomes. *Molecules* **2011**, *16*, 583−589.
(7) Kuo, Y. F.; Su, Y. Z.; Tseng, Y. H.; Wang, S. Y.; Wang, H. M.; Chueh, P. J. Flavokawain B, a novel chalcone from *Alpinia pricei* Hayata with potent apoptotic activity: Involvement of ROS and GADD153 upstream of mitochondria-dependent apoptosis in HCT116 cells. *Free Radic. Biol. Med.* **2010**, *49*, 214−226.
(8) Tang, Y.; Li, X.; Liu, Z.; Simoneau, A. R.; Xie, J.; Zi, X. Flavokawain B, a kava chalcone, exhibits robust apoptotic mechanisms on androgen receptor-negative, hormone-refractory prostate cancer cell lines and reduces tumor growth in a preclinical model. *Int. J. Cancer.* **2010**, *127*, 1758−1768.
(9) Mohamad, A. S.; Akhtar, M. N.; Zakaria, Z. A.; Perimal, E. K.; Khalid, S.; Mohd, P. A.; Khalid, M. H.; Israf, D. A.; Lajis, N. H.; Sulaiman, M. R. Antinociceptive activity of a synthetic chalcone, flavokawin B on chemical and thermal models of nociception in mice. *Eur. J. Pharmacol.* **2010**, *647*, 103−109.
(10) Peters, T., Jr. Serum albumin. *Adv. Protein Chem.* **1985**, *37*, 161−245.
(11) Petitpas, I.; Bhattacharya, A. A.; Twine, S.; East, M.; Curry, S. Crystal structure analysis of warfarin binding to human serum albumin. *J. Biol. Chem.* **2001**, *276*, 22804−22809.
(12) Kragh-Hansen, U.; Chuang, V. T. G.; Otagiri, M. Practical aspects of the ligand-binding and enzymatic properties of human serum albumin. *Biol. Pharm. Bull.* **2002**, *6*, 695−704.
(13) Curry, S.; Mandelkov, H.; Brick, P.; Franks, N. Crystal structure of human serum albumin complexed with fatty acid reveals an asymmetric distribution of binding sites. *Nat. Struct. Biol.* **1998**, *5*, 827−835.
(14) Sudlow, G.; Birkett, D. J.; Wade, D. N. The characterization of two specific drug binding sites on human serum albumin. *Mol. Pharmacol.* **1975**, *11*, 824−832.
(15) Wallevik, K. Reversible denaturation of human serum albumin by pH, temperature and guanidine hydrochloride. *J. Biol. Chem.* **1973**, *245*, 2650−2655.
(16) Twine, S. M.; Gore, M. G.; Morton, P.; Fish, B. C.; Lee, A. G.; East, J. M. Mechanism of binding of warfarin enantiomers to recombinant domains of human albumin. *Arch. Biochem. Biophys.* **2003**, *414*, 83−90.
(17) Faizul, F. M.; Kadir, H. A.; Tayyab, S. Spectroscopic studies on the binding of bromocresol purple to different serum albumins and its bilirubin displacing action. *J. Photochem. Photobiol. B.* **2008**, *90*, 1−7.
(18) Jacobsen, J.; Wennberg, R. P. Determination of unbound bilirubin in the serum of newborns. *Clin. Chem.* **1974**, *20*, 783−789.
(19) Kumar, Y.; Tayyab, S.; Muzammil, S. Molten-globule like partially folded states of human serum albumin induced by fluoro and alkyl alcohols at low pH. *Arch. Biochem. Biophys.* **2004**, *426*, 3−10.
(20) Lakowicz, J. R. *Principles of fluorescence spectroscopy*, 3rd ed.; Plenum Press: New York, 2006; pp 443−516.
(21) Yue, Y.; Zhang, Y.; Li, Y.; Zhu, J.; Qin, J.; Chen, X. Interaction of nobiletin with human serum albumin studied using optical spectroscopy and molecular modeling methods. *J. Lumin.* **2008**, *128*, 513−520.
(22) Pedretti, A.; Villa, L.; Vistoli, G. VEGA: a versatile program to convert, handle and visualize molecular structure on Windows-based PCs. *J. Mol. Graph. Model.* **2002**, *21*, 47−49.
(23) Dewar, M. J. S.; Zoebisch, E. G.; Healy, E. F.; Stewart, J. J. P. Development and use of quantum molecular models. 75. Comparative tests of theoretical procedures for studying chemical reactions. *J. Am. Chem. Soc.* **1985**, *107*, 3902−3909.
(24) Goodsell, D. S.; Morris, G. M.; Olson, A. J. Automated docking of flexible ligands: Applications of AutoDock. *J. Mol. Recognit.* **1999**, *9*, 1−5.
(25) Sanner, M. H. Python: A programming language for software integration and development. *J. Mol. Graph. Model.* **1999**, *17*, 57−61.
(26) Berman, H. M.; Westbrook, J.; Feng, Z.; Gilliland, G.; Bhat, T. N.; Weissig, H.; Shindyalov, I. N.; Bourne, P. E. The Protein Data Bank. *Nucleic Acids Res.* **2000**, *28*, 235−242.
(27) Muzammil, S.; Kumar, Y.; Tayyab, S. Molten globule-like state of human serum albumin at low pH. *Eur. J. Biochem.* **1999**, *266*, 26−32.
(28) Kalanur, S. S.; Seetharamappa, J.; Kalalbandi, V. K. A. Characterization of interaction and the effect of carbamazepine on the structure of human serum albumin. *J. Pharm. Biomed. Anal.* **2010**, *53*, 660−666.
(29) Khanna, N. C.; Tokuda, M.; Waisman, D. M. Conformational changes induced by binding of divalent cations to calregulin. *J. Biol. Chem.* **1986**, *261*, 8883−8887.
(30) Silva, D.; Cortez, C. M.; Louro, S. R. W. Chlorpromazine interactions to sera albumins: A study by the quenching of fluorescence. *Spectrochim. Acta A* **2004**, *60*, 1215−1223.
(31) Zhang, G.; Zhao, N.; Wang, L. Fluorescence spectrometric studies on the binding of puerarin to human serum albumin using warfarin, ibuprofen and digitoxin as site markers with the aid of chemometrics. *J. Lumin.* **2011**, *131*, 2716−2724.
(32) Varlan, A.; Hillebrand, M. Bovine and human serum albumin interactions with 3-carboxyphenoxathiin studied by fluorescence and circular dichroism spectroscopy. *Molecules* **2010**, *15*, 3905−3919.
(33) Ware, W. R. Oxygen quenching of fluorescence in solution: An experimental study of the diffusion process. *J. Phys. Chem.* **1962**, *66*, 455−458.
(34) Pan, X.; Liu, R.; Qin, P.; Wang, L.; Zhao, X. Spectroscopic studies on the interaction of acid yellow with bovine serum albumin. *J. Lumin.* **2010**, *130*, 611−617.
(35) Ross, P. D.; Rekharsky, M. V. Thermodynamics of hydrogen bond and hydrophobic interactions in cyclodextrin complexes. *Biophys. J.* **1996**, *71*, 2144−2154.
(36) Olsson, T. S. G.; Williams, M. A.; Pitt, W. R.; Ladbury, J. E. The thermodynamics of protein−ligand interaction and solvation: Insights for ligand design. *J. Mol. Biol.* **2008**, *384*, 1002−1017.
(37) Ross, P. D.; Subramaniam, S. Thermodynamics of protein association reactions: Forces contributing to stability. *Biochemistry* **1981**, *20*, 3096−3102.
(38) Zaroog, M. S.; Tayyab, S. Formation of molten globule-like state during acid denaturation of *Aspergillus niger* glucoamylase. *Process Biochem.* **2012**, *47*, 775−784.
(39) Kragh-Hansen, U. Molecular aspects of ligand binding to serum albumin. *Pharmacol. Rev.* **1981**, *33*, 17−53.
(40) Lupidi, G.; Scire, A.; Camaioni, E.; Khalife, K. H.; De Sanctis, G.; Tanfani, F.; Damiani, E. Thymoquinone, a potential therapeutic agent of *Nigella sativa*, binds to site I of human serum albumin. *Phytomedicine* **2010**, *17*, 714−720.
(41) Lohner, K.; Sen, A. C.; Prankerd, R.; Esser, A. F.; Perrin, J. H. Effects of drug-binding on the thermal denaturation of human serum albumin. *J. Pharm. Biomed. Anal.* **1994**, *12*, 1501−1505.
(42) Trynda-Lemiesz, L. Paclitaxel−HSA interaction. Binding sites on HSA molecule. *Bioorg. Med. Chem.* **2004**, *12*, 3269−3275.